

PHYSICAL REVIEW A

ATOMIC, MOLECULAR, AND OPTICAL PHYSICS

THIRD SERIES, VOLUME 51, NUMBER 2

FEBRUARY 1995

RAPID COMMUNICATIONS

The Rapid Communications section is intended for the accelerated publication of important new results. Since manuscripts submitted to this section are given priority treatment both in the editorial office and in production, authors should explain in their submittal letter why the work justifies this special handling. A Rapid Communication should be no longer than 4 printed pages and must be accompanied by an abstract. Page proofs are sent to authors.

Precise atomic radiative lifetime via photoassociative spectroscopy of ultracold lithium

W. I. McAlexander,¹ E. R. I. Abraham,¹ N. W. M. Ritchie,¹ C. J. Williams,² H. T. C. Stoof,^{1,3} and R. G. Hulet¹

¹Department of Physics and Rice Quantum Institute, Rice University, Houston, Texas 77251

²James Franck Institute, University of Chicago, Chicago, Illinois 60637

³University of Utrecht, Institute for Theoretical Physics, 3508 TA Utrecht, The Netherlands

(Received 1 August 1994)

We have obtained spectra of the high-lying vibrational levels of the $1^3\Sigma_g^+$ state of ${}^6\text{Li}_2$ via photoassociation of ultracold ${}^6\text{Li}$ atoms confined in a magneto-optical trap. The $1^3\Sigma_g^+$ state of the diatomic molecule correlates to a $2S_{1/2}$ state atom plus a $2P_{1/2}$ state atom. The long-range part of the molecular interaction potential for this state depends on the $2P$ atomic radiative lifetime. By calculating the energy eigenvalues of a model potential for the $1^3\Sigma_g^+$ state and fitting them to the experimentally measured vibrational levels, we have extracted a value for the $2P$ lifetime of 26.99 ± 0.16 ns. The precision is currently limited by the accuracy of a region of the model potential provided by *ab initio* calculations.

PACS number(s): 32.70.Fw, 32.80.Pj, 34.20.Cf, 34.50.Rk

Photoassociation of laser-cooled trapped atoms is a powerful spectroscopic technique for probing high-lying molecular vibrational states [1–3]. We use this technique to study the long-range interatomic potential of the first excited state of ${}^6\text{Li}_2$. This resonant dipole-dipole interaction depends on the $2P$ atomic lithium radiative lifetime [4]. Methods to extract long-range potential coefficients, assuming the asymptotic long-range form of the potential, have been developed previously [5] and have been applied to ultracold photoassociation spectra [2,3]. However, in those investigations the details of the potential are not accounted for, and the accuracy of the resulting long-range coefficients is only a few percent. We are able to extract a more precise value for the long-range potential coefficient, and therefore, the atomic radiative lifetime by fitting a model of the full interaction potential to the observed photoassociation spectrum.

Atomic radiative lifetimes are sensitive tests of atomic theory calculations, whose accuracies have improved dramatically in the past few years. Because of its relative simplicity, lithium is an important test case for atomic theory; methods must be capable of accurately representing lithium before the properties of heavier, more complicated atoms can reasonably be calculated. A recent state-of-the-art, relativistic all-order many-body perturbation-theory calculation of the radiative lifetime of the $2P$ state of lithium has an expected

uncertainty of 0.05% [6]. Experimentally, the measurement of the lithium $2P$ lifetime by Gaupp, Kuske, and Andr a, with a one standard-deviation uncertainty of 0.15%, is the most precisely stated measurement of any radiative lifetime [7]. Unfortunately, the theoretical value differs from the experimental one by more than 0.7%, or more than four standard deviations. Clearly, the resolution of this discrepancy is a high priority.

The experiment uses a six-beam magneto-optical trap (MOT) [8] to produce an ultracold lithium vapor [9]. A 500-mW probe laser beam with a Gaussian beam waist ($1/e^2$ radius) of $500 \mu\text{m}$ is directed through and retro-reflected back through the trapped atom cloud to induce photoassociation. As the probe is tuned to the red of the $2S_{1/2}$ - $2P_{1/2}$ atomic transition, it can excite colliding ground-state atoms into various high-lying vibrational levels of the molecular excited-state manifold. These newly formed diatomic molecules decay into a bound ground state of the molecule or into a dissociative continuum of two ground-state atoms that may gain enough kinetic energy to escape the trap. These combined processes result in an observable reduction in trap-laser-induced fluorescence, which is monitored by a photodiode. Vibrational levels up to 3 THz (100 cm^{-1}) red of the $2S_{1/2}$ - $2P_{1/2}$ atomic transition have been observed in this manner (Fig. 1) [10].

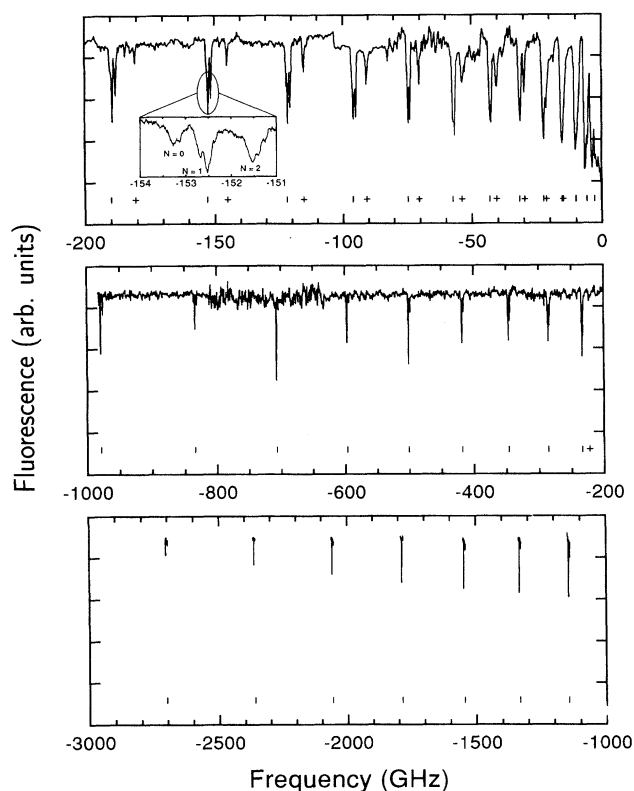


FIG. 1. Trap-laser-induced atomic fluorescence versus probe laser frequency detuning giving the photoassociation spectrum of ${}^6\text{Li}_2$. The frequency scale is relative to the $2S_{1/2}-2P_{1/2}$ atomic resonance frequency. Two distinct series of vibrational levels are observed. The series observable over the entire frequency range is assigned to the $1^3\Sigma_g^+$, while the series terminating near -200 GHz detuning corresponds to the $1^1\Sigma_u^+$ potential. The “s” correspond to the calculated eigenvalues of the $1^3\Sigma_g^+$ potential and range from $v=56$ to 84 while the “+”s indicate the calculated eigenvalues for the $1^1\Sigma_u^+$ potential. Since the data were taken at different times under somewhat different conditions, the relative signal sizes are the result of a combination of molecular and experimental effects. The inset shows rotational structure arising from $N=0, 1,$ and 2 . Partially resolved hyperfine structure is also evident from the inset.

At ultralow temperatures (≤ 1 mK) the spectral broadening due to the distribution of unbound ground-state energies can be comparable to the natural width. In addition, the spectra for lithium, unlike those of the other alkali species, are rotationally uncomplicated since only one or two partial waves contribute. Consequently, the spectra are simple with largely resolved hyperfine structure (see Fig. 1 inset). Photoassociation spectra have been obtained for both ${}^7\text{Li}_2$ and ${}^6\text{Li}_2$ [10]. However, the ${}^6\text{Li}_2$ spectrum is used for the lifetime extraction analysis since the ${}^6\text{Li}$ hyperfine interaction is sufficiently small, the atomic ground-state hyperfine splitting of ${}^6\text{Li}$ is only 228 MHz, that it may be neglected at the current level of precision. There are two distinct vibrational series observable in Fig. 1 that correspond to the two attractive Hund’s case (b) excited molecular states, $1^1\Sigma_u^+$ and $1^3\Sigma_g^+$, asymptotic with the $2S_{1/2}+2P_{1/2}$ atomic states. Three rotational lines ($N=0, 1,$ and 2) are visible in the

$1^3\Sigma_g^+$ series (see Fig. 1 inset); we use the $N=0$ line in the analysis.

The basis of the analysis involves the construction of a model potential for the excited molecular state. Energy eigenvalues of this potential are calculated numerically and compared with the observed spectrum. The analysis focuses on the $1^3\Sigma_g^+$ series whose levels represent the majority of the observed spectral features. The interaction potential is constructed from a combination of experimental and theoretical information, depending on the interatomic separation R . For $R > 20a_0$, where a_0 is the Bohr radius, the potential is approximated analytically. The dominant molecular interaction in this range is due to a resonant dipole. This interaction follows a functional form of $-C_3/R^3$, where C_3 is a constant proportional to the square of the dipole matrix element, which in turn is inversely proportional to the $2P$ atomic radiative lifetime τ [4]:

$$C_3 = \frac{3\hbar}{2\tau} \left(\frac{\lambda}{2\pi} \right)^3. \quad (1)$$

Dispersion terms of the form $-C_6/R^6 - C_8/R^8$ are also included, where $C_6 = 1927$ a.u. and $C_8 = 2.3 \times 10^5$ a.u., with uncertainties of $\pm 20\%$ [11], although their contributions are small for $R > 20a_0$. At very long range, the Hund’s case (b) $1^3\Sigma_g^+$ potential correlates to both the 0_g^- and 1_g Hund’s case (c) potentials, which depend on both C_3 and the P state fine-structure interval [12].

For R between $4.7a_0$ and $7.8a_0$, Rydberg-Klein-Rees (RKR) points for the $1^3\Sigma_g^+$ potential have been determined from Fourier transform spectroscopy of the $1^3\Sigma_g^+ - a^3\Sigma_u^+$ transition [13]. The original uncertainty in these points of ± 1.2 cm^{-1} has been improved by subsequent analysis to ± 0.3 cm^{-1} [14]. This experimentally determined region of the potential is certainly the most accurately known region. For both the inner wall ($R < 4.7a_0$) and the region between $7.8a_0$ and $20a_0$, two different, highly regarded *ab initio* potentials are used. The calculated potentials of Schmidt-Mink, Müller, and Meyer (SMM) produce the best comparison with spectroscopically known constants [15]. The average of two *ab initio* calculations by Konowalow and co-workers (KC), for which the expected errors are of opposite sign, is also expected to be a reasonable approximation to the true potential [16]. Although this “composite” potential (KC) does not agree as well as SMM with the experimental RKR potential in the region near the potential minimum [$(4.7-7.8)a_0$], the two potentials making up the KC were designed to be accurate over a larger range of R [16], where RKR points are unavailable. The various regions making up the model potential are joined smoothly using a cubic spline fit. Vibrational quantum numbers v were assigned by comparing the calculated eigenvalues with the data. The assignments did not change when varying each component of the model potential by its respective uncertainty, and the assignments are isotopically consistent [10].

Even though the analysis is made with the $N=0$ rotational levels, there is a small rotational contribution to the energies due to coupling of electronic and rotational angular momenta. This term, equal to $\langle L^2 \rangle / (2\mu R^2)$, where μ is the reduced mass, was added to the model potential in all regions, except that defined by the RKR points. This represents

TABLE I. Best-fit values of C_3 and corresponding χ^2 's for the four model potentials arising from the combinations of the two *ab initio* theories (SMM [15] and KC [16]) in the regions $R < 4.7a_0$ and $7.8a_0 < R < 20a_0$.

$R < 4.7a_0$	$7.8a_0 < R < 20a_0$	C_3 (a.u.)	χ^2 (10^{-5})
SMM	SMM	11.11	30
SMM	KC	11.05	2.8
KC	SMM	11.11	25
KC	KC	11.04	2.1

a first-order correction to the adiabatic Born-Oppenheimer approximation and only becomes significant compared to other contributions to the potential at long range. We calculate $\langle L^2 \rangle = 2\hbar^2$, when evaluated in the long-range asymptotic basis. Exclusion of this term changes the resulting C_3 by only 0.07%, setting the scale for nonadiabatic effects.

In order to extract the atomic radiative lifetime, the data are fit to a potential in which C_3 is a free parameter. For a given model potential, C_3 is determined by minimizing the χ^2 function:

$$\chi^2 = \sum_v \frac{(E_v^{(e)} - E_v^{(t)})^2}{E_v^{(e)2}}, \quad (2)$$

where the sum extends over the vibrational levels v , $E_v^{(e)}$ and $E_v^{(t)}$ are the experimentally and theoretically determined energies, respectively, and where $E_v^{(t)}$ is a function of C_3 . The model potential is expected to be less accurate for the longer-range least-bound states because of the neglected effects of radiation retardation [17] and hyperfine interactions. For these reasons, the levels $v = 80$ to 86 are not included in the analysis. Also, the most deeply bound $N = 0$ level observed is $v = 59$. The levels included in the fit have outer classical turning points ranging from $34a_0$ to $124a_0$. For this range of vibrational states, the potential difference between the 1_g and 0_g^- Hund's case (c) states is insignificant at the present level of precision.

Most of the difference between the SMM and KC *ab initio* potentials in the range from $12a_0$ – $20a_0$ is caused by

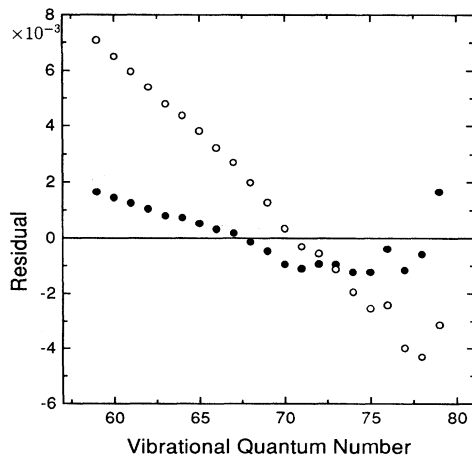


FIG. 2. Residuals, $(E_v^{(e)} - E_v^{(t)})/E_v^{(e)}$, of best fits to C_3 using different *ab initio* calculations for the potential inner wall and the $7.8a_0$ – $20a_0$ region. \circ , SMM [15]; \bullet , KC [16].

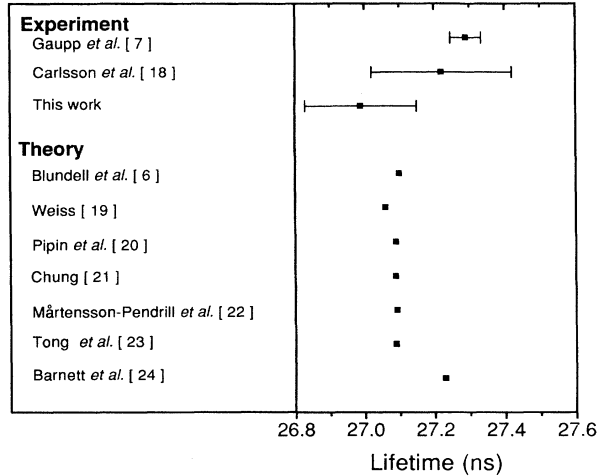


FIG. 3. Comparison of recent measurements and some theoretical calculations of the Li $2P$ radiative lifetime. The error bars given for the Gaupp *et al.* and Carlsson *et al.* measurements correspond to one standard deviation, while the error bar for the present experiment is chosen to encompass the results of all model potentials considered. We assume that differences in lifetime between ${}^6\text{Li}$ and ${}^7\text{Li}$ and between the $2P_{1/2}$ and $2P_{3/2}$ states is insignificant at the present level of precision.

differences in their respective C_3 values. SMM calculate $C_3 = 11.02$ a.u., while KC find $C_3 = 11.16$ a.u. At small R it is not valid to separate the contributions to the potential using long-range coefficients. However, at $R = 12a_0$, the resonant dipole interaction still accounts for more than 85% of the total interaction energy. Therefore, this contribution is accounted for in the fit by subtracting the resonant dipole contribution from each of the *ab initio* potentials for $R > 12a_0$ and adding back the term $-C_3/R^3$, where C_3 is the fitted parameter.

Despite the fact that the model potential is good enough to unambiguously assign vibrational quantum numbers, the accuracy of the fit is limited by systematic uncertainties in the data. The fit is most sensitive to which *ab initio* theory is used for the $7.8a_0$ – $20a_0$ region (see Table I). The best-fit value for C_3 varies by 0.6% depending on whether the SMM or KC theory is used. However, the minimized value of χ^2 is significantly smaller for the KC potential than for the SMM theory, indicating that the KC potential is superior in the $7.8a_0$ – $20a_0$ range. The residuals of the fits (Fig. 2) show that neither potential is ideal, but imply that the actual potential lies closer to the KC potential. The resulting C_3 also depends on the inner wall potential, differing by 0.1%, depending on which *ab initio* theory is used for $R < 4.7a_0$. The fractional variation in C_3 resulting from shifting C_6, C_8 , all the data points, or all the RKR points by their respective uncertainties is 5×10^{-4} , 1×10^{-4} , 2×10^{-4} , and $< 5 \times 10^{-5}$, respectively.

Since some of the potential models result in a better fit to the data than others, the best estimate of C_3 is given by a weighted average, where the weighing factors are $(\chi^2)^{-1}$. A rigorous estimate of the uncertainty is impossible, since the

model potentials are not “normally” distributed. However, our best estimate of the uncertainty is a value that encompasses the C_3 resulting from all model potentials considered. Using a weighted average of the four combinations of the two *ab initio* potentials in the two regions given by Table I, we obtain $C_3 = 11.048 \pm 0.066$ a.u. This corresponds to a radiative lifetime for the $2P$ state of 26.99 ± 0.16 ns. A fit to the energy differences between adjacent vibrational levels, rather than to the absolute energies, was also made, and the results are nearly identical. A similar analysis was used to examine the other observed vibrational series corresponding to the $1^3\Sigma_g^+$ state of ${}^7\text{Li}_2$ as well as the $1^1\Sigma_u^+$ state of ${}^6\text{Li}_2$ and ${}^7\text{Li}_2$. While not as accurate, the extracted lifetimes were consistent with the presented analysis for ${}^6\text{Li}_2$ and fall within our stated uncertainty.

Figure 3 shows our result, in comparison with recent experimental and several recent theoretical determinations of the lifetime [6,7,18–24]. The recent quantum Monte Carlo calculation of Barnett and co-workers [24] agrees with previous experimental work, but disagrees with the other calculations. Our result is consistent with the other theoretical calculations and the measurement of Carlsson and Sturesson [18]. While our estimated uncertainty lies outside the range of Gaupp, Kuske, and Andr a’s experimental result [7], a further reduction in uncertainty is necessary before drawing a definitive conclusion. The potential models we use do not necessarily bracket the true adiabatic potential, but they do indicate the amount of systematic uncertainty present in the *ab initio* regions of the model.

It is possible to extract C_3 from the data by a long-range analysis of the energy differences between adjacent vibrational levels, assuming the potential is purely of the long-range form [5]. Although this procedure gives a similar value of C_3 , it is sensitive to which levels are included in the analysis since the potential does not vary strictly as R^{-3} , and thus is not as accurate. Such a procedure has recently been applied to the ultracold photoassociation spectra of Na [2] and of Rb [3]. In both cases, the accuracy was limited to several percent due to the neglect of the non- R^{-3} part of the potential, and complications due to the hyperfine interaction.

The spectral resolution of the photoassociation data presented here is such that an order-of-magnitude reduction in the uncertainty of the lifetime determination could be achieved with a more accurate potential, especially in the $8a_0$ – $20a_0$ region. It may be possible to extend the number of observed lower-lying vibrational levels above those presently known by a triple-resonance technique [25], in order to extend the RKR potential higher in the well. Clearly, the lifetime analysis would also benefit from improvements in *ab initio* theory that focus on this range. In order to realize the full precision inherent in the data it will also be necessary to account for hyperfine, retardation, and non-Born-Oppenheimer effects in the analysis.

The work has been supported by the National Science Foundation, the Texas Advanced Technology Program, and the Welch Foundation. W.I.M. received support from the Fannie and John Hertz Foundation.

-
- [1] H. R. Thorsheim, J. Weiner, and P. S. Julienne, *Phys. Rev. Lett.* **58**, 2420 (1987); M. E. Wagshul, K. Helmerson, P. D. Lett, S. L. Rolston, and W. D. Phillips, *ibid.* **70**, 2074 (1993); V. Bagnato, L. Marcassa, C. Tsao, Y. Wang, and J. Weiner, *ibid.* **70**, 3225 (1993); J. D. Miller, R. A. Cline, and D. J. Heinzen, *ibid.* **71**, 2204 (1993); L. P. Ratliff, M. E. Wagshul, P. D. Lett, S. L. Rolston, and W. D. Phillips, *J. Chem. Phys.* **101**, 2638 (1994); C. J. Williams and P. S. Julienne, *ibid.* **101**, 2634 (1994); R. Napolitano, J. Weiner, C. J. Williams, and P. S. Julienne, *Phys. Rev. Lett.* **73**, 1352 (1994).
- [2] P. D. Lett, K. Helmerson, W. D. Phillips, L. P. Ratliff, S. L. Rolston, and M. E. Wagshul, *Phys. Rev. Lett.* **71**, 2200 (1993).
- [3] R. A. Cline, J. D. Miller, and D. J. Heinzen, *Phys. Rev. Lett.* **73**, 632 (1994).
- [4] G. W. King and J. H. Van Vleck, *Phys. Rev.* **55**, 1165 (1939).
- [5] R. J. Le Roy and R. B. Bernstein, *J. Chem. Phys.* **52**, 3869 (1970); W. C. Stwalley, *Chem. Phys. Lett.* **6**, 241 (1970).
- [6] S. A. Blundell, W. R. Johnson, Z. W. Liu, and J. Sapirstein, *Phys. Rev. A* **40**, 2233 (1989).
- [7] A. Gaupp, P. Kuske, and H. J. Andr a, *Phys. Rev. A* **26**, 3351 (1982).
- [8] E. L. Raab, M. Prentiss, A. Cable, S. Chu, and D. E. Pritchard, *Phys. Rev. Lett.* **59**, 2631 (1987).
- [9] N. W. M. Ritchie, E. R. I. Abraham, and R. G. Hulet, *Laser Phys.* **4**, 1066 (1994).
- [10] The complete spectroscopic data will be presented in the future.
- [11] B. Bussery and M. Aubert-Fr econ, *J. Chem. Phys.* **82**, 3224 (1985).
- [12] M. Movre and G. Pichler, *J. Phys. B* **10**, 2631 (1977).
- [13] C. Linton, T. L. Murphy, F. Martin, R. Bacis, and J. Verges, *J. Chem. Phys.* **91**, 6036 (1989).
- [14] W. T. Zemke and W. C. Stwalley, *J. Phys. Chem.* **97**, 2053 (1993).
- [15] I. Schmidt-Mink, W. M uller, and W. Meyer, *Chem. Phys.* **92**, 263 (1985).
- [16] D. D. Konowalow and J. L. Fish, *Chem. Phys.* **84**, 463 (1984); M. L. Olson and D. D. Konowalow, *ibid.* **21**, 393 (1977); D. D. Konowalow and J. L. Fish, *ibid.* **77**, 435 (1983).
- [17] W. J. Meath, *J. Chem. Phys.* **48**, 227 (1968).
- [18] J. Carlsson and L. Sturesson, *Z. Phys. D* **14**, 281 (1989).
- [19] A. W. Weiss, *Can. J. Chem.* **70**, 456 (1992).
- [20] J. Pipin and D.M. Bishop, *Phys. Rev. A* **45**, 2736 (1992).
- [21] K. T. Chung, in *Sixth International Conference on The Physics of Highly Charged Ions*, edited by P. Richard, M. Stockli, C. L. Cocke, and C. D. Lin, AIP Conf. Proc., No. 274 (AIP, New York, 1993), p. 381.
- [22] A.-M. M artensson-Pendrill and A. Ynnerman, *Phys. Scr.* **41**, 329 (1990).
- [23] M. Tong, P. J onsson, and C. Froese Fisher, *Phys. Scr.* **48**, 446 (1993).
- [24] R. N. Barnett, P. J. Reynolds, and W. A. Lester Jr., *Int. J. Quantum Chem.* **42**, 837 (1992); R. N. Barnett, E. M. Johnson, and W. A. Lester Jr. (unpublished).
- [25] A. M. Lyyra, H. Wang, T.-J. Whang, W. C. Stwalley, and L. Li, *Phys. Rev. Lett.* **66**, 2724 (1991).